Making a Connection: Direct Binding between Keratin Intermediate Filaments and Desmosomal Proteins

Panos D. Kouklis, Elizabeth Hutton, and Elaine Fuchs

Howard Hughes Medical Institute, Department of Molecular Genetics and Cell Biology, The University of Chicago, Chicago, Illinois 60637

Abstract. In epidermal cells, keratin intermediate filaments connect with desmosomes to form extensive cadherin-mediated cytoskeletal architectures. Desmoplakin (DPI), a desmosomal component lacking a transmembrane domain, has been implicated in this interaction, although most studies have been conducted with cells that contain few or no desmosomes, and efforts to demonstrate direct interactions between desmoplakin and intermediate filaments have not been successful. In this report, we explore the biochemical nature of the connections between keratin filaments and desmosomes in epidermal keratinocytes. We show that the carboxy terminal "tail" of DPI associates directly with the amino terminal "head" of type II epidermal keratins, including K1, K2, K5, and K6. We have engineered and purified recombinant K5 head and DPI tail, and we demonstrate direct interaction in vitro by solution-binding assays and by ligand blot assays. This marked association is not seen with simple epithelial type II keratins, vimentin, or with type I keratins, providing a possible explanation for the greater stability of the epidermal keratin filament architecture over that of other cell types. We have identified an 18-amino acid residue stretch in the K5 head that is conserved only among type II epidermal keratins and that appears to play some role in DPI tail binding. This finding might have important implications for understanding a recent point mutation found within this binding site in a family with a blistering skin disorder.

MANY cell types distinguish self from nonself by virtue of cell surface adherens junctions involving members of the cadherin family (for reviews, see Kemler, 1993; Garrod, 1993; Franke et al., 1992). While a number of cell types stabilize homophilic cadherin-mediated associations by connecting to an actin cytoskeletal network (Pasdar et al., 1991; Pasdar and Nelson, 1988), others, including heart muscle and epidermis, orchestrate cell adhesion through desmosomes, which connect to intermediate filament (IF)[1] networks (Garrod, 1993).

Desmosomes are symmetrical membranous plaques that are several microns in diameter and ~100 nm thick. Each half of the desmosome is derived from an adjacent cell, and IFs from both cells appear to loop through the cytoplasmic peripheries of the structure (Kelly, 1966). Desmosomes contain two subtypes of the transmembrane glycoprotein superfamily of cadherins, desmogleins (Dsgs), and desmocollins (Dscs), each of which are encoded by at least three differentially expressed genes (for review, see Koch et al., 1992; Arnemann et al., 1993). Typical of cadherin-mediated junctions, desmosomes also contain a member of the catenin family, plakoglobin (Cowin et al., 1986; Gumbiner and McCrea, 1993). Unique to desmosomes and not seen in actin-mediated adherens junctions are two proteins, desmoplakin I and II (DPI and DPII), which seem to be splice variants encoded by a single gene that is widely expressed in cells that possess desmosomes (Green et al., 1988; Angst et al., 1990). In contrast to the desmosomal cadherins, desmoplakin has no obvious transmembrane domain, and it appears to be a cytoplasmic protein (Green et al., 1990, 1992). Antibody studies indicate that desmoplakin resides in the inner plaque zone, between the plaque and the intermediate filaments (Miller et al., 1987; Jones and Grelling, 1989).

Based on its location and on the absence of an obvious homologue in actin-mediated, cell–cell adherens junctions, desmoplakin has emerged as a leading candidate for making the molecular connections between desmosomes and IFs. As visualized by electron microscopy of rotary shadowed images, purified DPI is a dimer that has a rodlike structure with folded or globular amino (head) and carboxy (tail) domains (O'Keefe et al., 1989). Although it was initially suggested that the rod domain of ~130 nm might represent a tail-to-tail

Address all correspondence to Elaine Fuchs, Howard Hughes Medical Institute, Department of Molecular Genetics and Cell Biology, The University of Chicago, 5841 S. Maryland Avenue, Room N314, MC1058, Chicago, IL 60637.

1. *Abbreviations used in this paper*: Dsgs, desmogleins; Dscs, desmocollins, DPI and DPII, desmoplakin I and II, respectively; ENDO LYS-C, endolysine protease; FPLC, fast protein liquid chromatography; HAP, hydroxyapatite; IB, inclusion body; IBF, inclusion body fractions; IF, intermediate filament; IPTG, isopropyl-β-thiogalactopyranoside; NTCB, 2-nitro-5-thiocyanatobenzoic acid.

association of DPI monomers (O'Keefe et al., 1989), secondary structure analysis of the DPI sequence predicts a coiled-coil rod of this size, with a smaller rod predicted for the DPII splice product (Green et al., 1990). DPI's head (>862 aa) and tail (851 aa) are identical in size and sequence to those of DPII (Green et al., 1990; Virata et al., 1992).

Truncated DPI molecules have been transiently expressed at very high levels in COS simple epithelial cells, which have few desmosomes, and in mouse fibroblasts, which have none (Stappenbeck and Green, 1992; Stappenbeck et al., 1993). In the absence of the NH_2-terminal head domain, DPI molecules were unable to associate with desmosomal plaques, and instead they colocalized with the endogenous IF network (Stappenbeck and Green, 1992; Stappenbeck et al., 1993). In both fibroblasts and in simple epithelial cells, this association was maintained as long as the COOH-terminal tail domain of DPI was present. However, when treated with a nonionic detergent, fibroblasts released the DPI rod-tail domain into the soluble fraction, whereas simple epithelial cells retained it with the cytoskeleton (Stappenbeck et al., 1993). From these data, it might be predicted that DPI associates more strongly with a simple epithelial keratin network than with a vimentin IF network.

Little is known about the precise nature of the association between the 851 amino acid residue DPI tail and IFs. While removal of 68 residues from the COOH-terminal end of the DPI tail obliterates the interaction, at least in simple epithelial cells, the 68-residue COOH terminus on its own is not sufficient for the association (Stappenbeck and Green, 1993). Even less is known about the IF sequences involved in this interaction, and efforts to identify a direct association between purified DPI and tongue epithelial keratins have been unsuccessful (O'Keefe et al., 1989). A priori, the failure to cosediment keratin IFs and purified DPI might seem to support the notion that the interaction might be indirect, rather than direct. However, these data do not resolve the issue, since (*a*) the extensive purification procedure that was used for desmoplakins required potentially denaturing buffers; (*b*) the NH_2-terminal domain of desmoplakin, when removed from its interactions with other desmosomal components, could adopt a new conformation which in turn prevents the association between the COOH-terminal domain of desmoplakin and IFs; and (*c*) the status of the COOH terminus of purified DPI, critical for IF association, was not determined.

In this report, we use epidermal keratinocytes, where desmosomes are abundant, to delve more deeply into the precise nature of this interaction. We present experiments that suggest that the interaction between DPI and epidermal keratins is a direct one involving the NH_2-terminal head domain of type II epidermal keratins and the COOH-terminal tail domain of DPI. We show that the association between the DPI tail and IFs is more prominent for epidermal keratin filaments than for simple epithelial keratin filaments or vimentin IFs. Finally, we have identified a segment of the head that is conserved among type II epidermal keratins and that seems to be involved in the binding to DPI. Our findings have important implications for understanding why a point mutation in the head of a type II epidermal keratin may lead to keratin network instability and epidermal cell fragility in a family with palmoplantar keratoderma (Kimonis, V., J. J. DiGiovanna, J.-M. Yang, S. Z. Doyle, S. J. Bale, and J. G. Compton. *J. Invest. Dermatol.* 102:545*a*).

Materials and Methods

Plasmid Constructs

phDPIrt. A 7-kb DPI/II genomic clone was isolated from a human genomic library in lambda Charon 4A, and it was cloned into the EcoRI site of plasmid Bluescript KS^+. This clone encodes the entire rod and all but 18 codons of the tail of DPI. A 2.5-kb cDNA clone containing 2 kb of 3′ coding sequence and 0.5 kb of 3′ nontranslated sequence of DPI was isolated from a human keratinocyte cDNA library in lambda gt11 (Clontech Laboratories, Palo Alto, CA). The two clones were combined using a unique BstEII site in the coding sequence, so that a complete rod and tail sequence was generated. This sequence was cloned into the EcoRI site of pKS^+ to generate phDPIrt. The sequences of these clones were identical to that of the previously published DPI (Green et al., 1990).

pFG·DPtail. A 3.2-kb NdeI-Klenow/SpeI fragment containing sequences extending from the proline codon 1863 to 0.3 kb 3′ of the TGA stop codon was subcloned in frame at the BglII-Klenow/XbaI site of the plasmid pECE-FLAG, a mammalian expression vector containing the SV-40 major early promoter and enhancer, followed by an ATG and sequences encoding the 9-amino acid residue FLAG epitope tag, followed by a polylinker region, followed by a 3′ untranslated and polyadenylation site from SV-40 (kindly provided by Dr. Magnus Pfahl, La Jolla Cancer Research Foundation, La Jolla, CA).

pET8c·DPtail. An NcoI site was created by PCR mutagenesis 5′ of the lysine codon 1987, and a fragment encoding the DP tail plus 0.5 kb of 3′ noncoding sequence was inserted at the NcoI/BamHI site of the pET8c bacterial vector (Studier and Moffatt, 1986).

pET22b·K5H and Mutants. Plasmid pETK5 (Coulombe and Fuchs, 1990) was digested with BglII to excise a 1.2-kb fragment containing sequences encoding the 164 amino acid residue K5 head domain plus four residues of helix 1A (for sequence, see Lersch et al., 1989). This fragment was then digested with ThaI, digested with XbaI, and finally ligated into the bacterial vector pET22b (Novagen, Inc., Madison, WI) at its XbaI/NotI sites (NotI site was blunted with Klenow). The resulting vector contained a T7 promoter, followed by the K5 head (the leader and signal peptidase sequence of pET22b were removed), followed by a six-codon histidine tag sequence, TGA stop codon, and T7 termination sequence.

Transfections and Immunofluorescence

SCC-13 human epidermal keratinocytes (K14+, K5+) were transiently transfected and subjected to double immunofluorescence as described previously (Albers and Fuchs, 1987). The antibodies used were a 1:100 dilution of guinea pig anti-human K5 (Lersch et al., 1989), 10 μg/ml of a mouse anti-FLAG M2 monoclonal antibody (IBI-Kodak, New Haven, CT), and a 1:20 dilution of affinity-purified rabbit anti-human DPI tail antiserum. The polyclonal anti-DPI tail antiserum was prepared by injecting rabbits with an initial 200-μg purified recombinant DPI tail, followed by two 200-μg boosts separated at 3-wk intervals.

Overlay Binding Assays

Protein levels were determined using the Bradford assay (1976). Purified DPI tail was biotinylated using the succinimide ester of biotin as described by Harlow and Lane (1988). The coupling occurs primarily through the free ε-amino groups of lysine residues. Briefly, 1 mg of DPI tail in 1 ml PBS was subjected to centrifugation at 25,000 *g* for 30 min, and the supernatant (~0.7 mg/ml) was combined with a solution of 1 mg/ml *N*-hydroxysuccinimide biotin in dimethyl sulfoxide such that the molar ratio of biotin/DPI tail was 1.5. After 4 h at room temperature, 2 μl of 1 M NH_4Cl was added, and the solution was incubated for another 10 min before extensive dialysis against 20 mM Tris-HCl, pH 7.2, to remove uncoupled biotin.

Ligand blotting assays were performed essentially as described by Merdes et al. (1991). 1-mm thick SDS-polyacrylamide gels were made using ultrapure electrophoresis reagents (Bio Rad Laboratories, Hercules, CA). After electrophoresis of duplicate gels, one gel was used for staining with Coomassie blue to visualize the proteins, and the other was transferred to nitrocellulose membranes (35 V for 2 h at room temperature) in a buffer containing 57.6 g glycine, 12.1 g Tris (base), 4 g SDS, and 800 ml methanol per 4 liters of solution. Blots were washed three times with buffer (0.9% [wt/vol] NaCl, 20 mM Tris-HCl, pH 7.3, 0.1% Tween 20, 1 mM $MgCl_2$, 1 mM dithiothreitol, 0.2% [wt/vol] gelatin [Sigma Chemical Co., St. Louis, MO], and 0.2 mM phenyl methyl sulfonyl fluoride) at room temperature. The blots were then probed with buffer containing 0.2 μg/ml biotinylated DPI tail at room temperature for 1–2 h. After extensive washing, blots were

incubated at 4°C for 1 h with horseradish peroxidase–coupled streptavidin (Boeringher-Mannheim Biochemicals, Indianapolis, IN). Blots were washed 4 × 15 min and were then developed by the ECL chemiluminescence kit (Amersham Corp., Arlington Heights, IL).

Fast Protein Liquid Chromatography (FPLC) Purification of Keratins, Filament Assembly, and Quantiation. Bacterially expressed keratins were isolated from inclusion bodies and purified by a Mono-Q anion exchange column (Coulombe and Fuchs, 1990). Keratins were concentrated by filtration through Centricon-10 units (Amicon, W. R. Grace & Co., Beverly, MA). K5 and K14 or corersponding mutants were mixed in a 1:1.05 ratio (K5:K14) and were purified as a heteromeric complex by FPLC. All buffers contained 10 mM β-mercaptoethanol and were at pH 7.5. Complexes were equilibrated by dialysis against the following buffers: (*a*) 9.5 M urea, 10 mM Tris·HCl (10 h at room temperature); (*b*) 4 M urea, 10 mM Tris·HCl (12 h, at room temperature); and (*c*) 1 M urea, 10 mM Tris·HCl (2 h at 4°C), (*d*) 5 mM Tris·HCl buffer (2 h at 4°C), twice.

Results

The DPI Tail Associates with Epidermal Keratin Networks In Vivo

Our first goal was to assess whether the DPI tail associates in vivo with epidermal keratin networks, as it appears to do with vimentin and simple epithelial keratin networks. We began our studies by adding an NH_2-terminal epitope "FLAG" tag fused in frame to 927 COOH-terminal amino acid residues of human DPI that we had isolated from a human keratinocyte λgt11 cDNA library (Fig. 1 *A*). The sequence included the short linker region spanning the α-helical rod domain and the tail, and in its entirety, was identical to that previously reported by Green et al. (1990). When expressed transiently in cultured epidermal keratinocytes or in COS simple epithelial cells, this expression vector, referred to as pFG·DPtail, produced a single species that could be detected at low levels in immunoblots incubated with a rabbit anti-DPI tail polyclonal antiserum and at high levels by an anti-FLAG antiserum (Fig. 1 *B*). In contrast to endogenous DPI and DPII (*open arrowheads*), ~80% of the DPI tail (*solid arrowhead*) in epidermal keratinocytes and nearly 100% of the DPI tail in COS cells were solubilized upon sonication in the presence of 1% Triton X-100 in PBS. Additionally, the level of expression of the DPI tail in transfected COS cells was estimated to be >100× its level in keratinocytes, as judged by the failure of anti-FLAG to detect the transgene product in keratinocyte extracts.

When transiently transfected into SCC-13 keratinocytes, pFG·DPtail decorated the epidermal keratin network (Fig. 2, *A* and *C*, anti-FG; *B* and *D*, anti-K5). Approximately 5% of cells were transfected. About 5–10% of these transfected epidermal keratinocytes displayed a collapsed or partially collapsed keratin filament network (Fig. 2, *A–D*). Often, the keratin network appeared unaffected, and in no case did the FG·DPtail colocalize with desmosomes (Fig. 2 *E*, anti-FG; and *F*, anti-DP). The lack of colocalization between the DPI tail and desmosomes was in agreement with Stappenbeck and Green (1992), who showed that the NH_2 terminus of DPI is required for its association with desmosomes in simple epithelial (COS) cells. Overall, however, the behavior of the DPI tail in keratinocytes was distinct from that seen in COS simple epithelial cells, where virtually all the transfected cells displayed a collapse of the keratin network (Stappenbeck and Green, 1992; Kouklis and Fuchs, data not shown). Presumably, the combination of closer to physiological levels of transgene expression, a more stable keratin network, and a larger number of anchoring desmosomes made the epidermal keratin IF network more resistant to collapse than the simple epithelial one.

It is possible that the association observed in vivo between the desmoplakin tail and the keratin IF network was disrupted by the cytoskeletal extraction procedure used in our

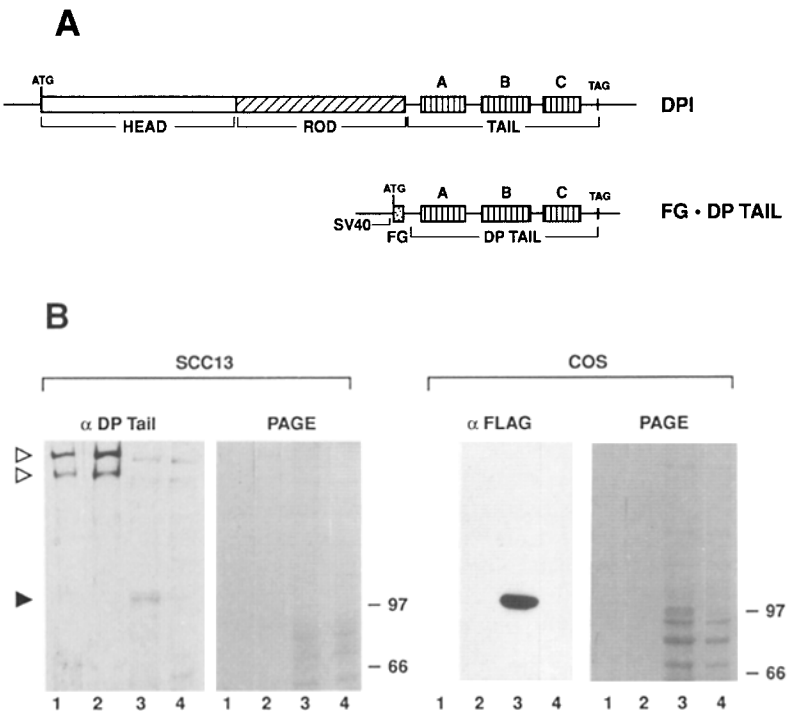

Figure 1. Detection of recombinant DPI tail in transiently transfected epithelial cells. (*A*) Shown at top is a stick figure depicting the predicted secondary structure for human DPI (Green et al., 1992). Beneath this structure is a diagram of the SV-40 promoter–based mammalian expression vector pFG·DPtail (see Materials and Methods for complete details). This vector was used to drive the expression of the FLAG epitope–tagged DPI tail in the human epidermal keratinocyte line SCC-13 and the monkey kidney simple epithelial cell line COS. (*B*) 48 (*COS*) or 65 (*SCC-13*) h after transfection with pFG·DPtail or the pECE-FLAG empty expression vector, cells were lysed with 1% Triton X100 in PBS and they were separated into soluble and pellet fractions by centrifugation at 12,000 *g*. Fractions were resolved by electrophoresis through 6% SDS PAGE gels and either stained with Coomassie blue or subjected to immunoblot analysis with either anti-DPI tail antiserum (*αDPtail*) or anti-FG antibody (*αFLAG*). Lanes *1* and *3*, pFG·DPtail transfected pellet and soluble fractions, respectively; lanes *2* and *4*, pECE-FLAG transfected pellet and soluble fractions, respectively. Note the presence of endogenous DPI/II bands (*open arrowheads*) and transgene product (*solid arrowhead*). Molecular mass standards are indicated in kilodaltons at right. Exposure times: SCC-13, 2 min; COS, 30 s.

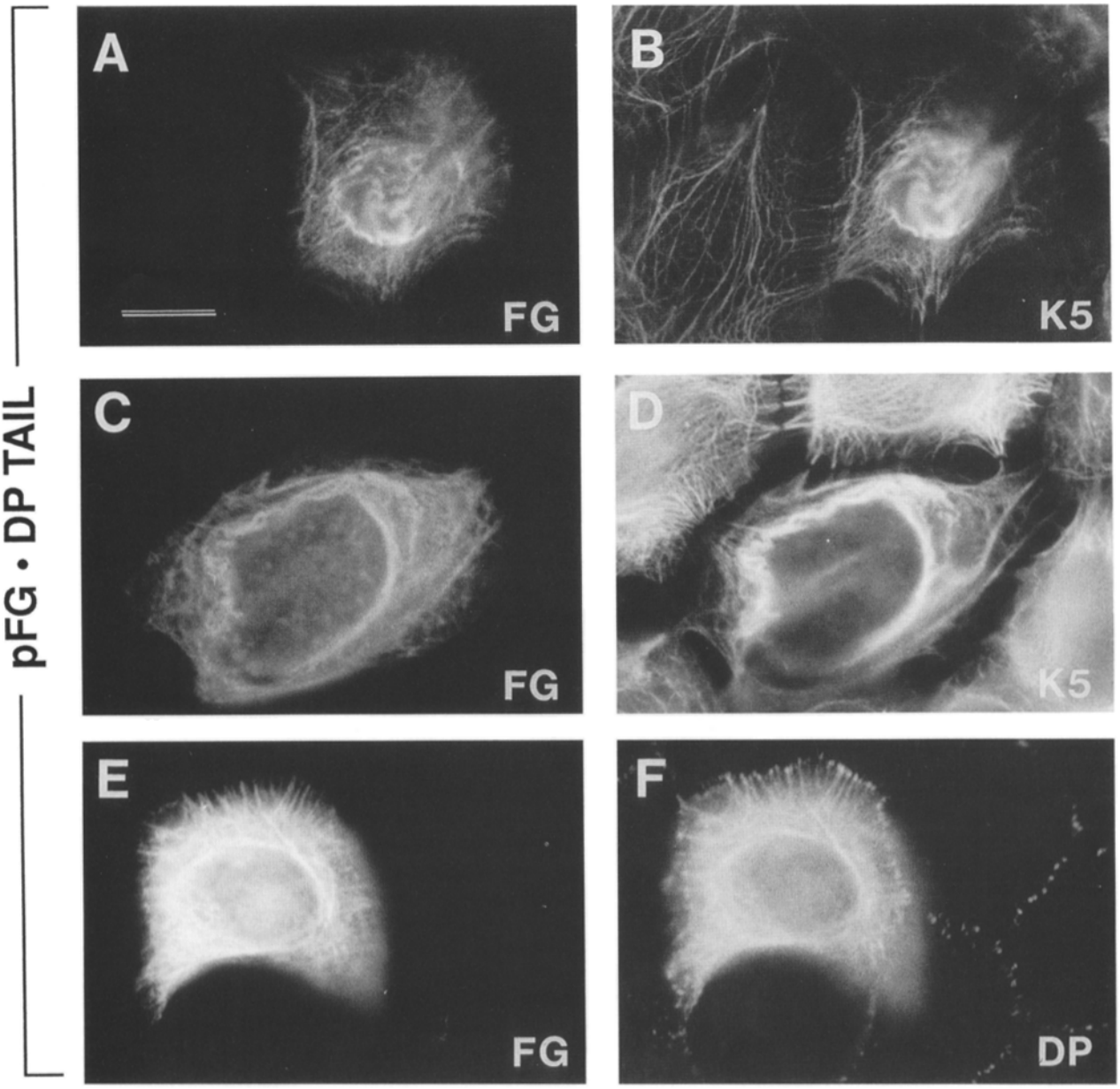

Figure 2. Colocalization of the DPI tail with the epidermal keratin network. Human epidermal keratinocytes (SCC-13) were transiently transfected with pFG·DPtail, and 65 h later, cells were fixed and processed for double immunofluorescence using a mouse monoclonal anti-FG antibody and either a guinea pig polyclonal antisera against human K5 COOH-terminal peptide or an affinity-purified rabbit polyclonal antisera against human DPI tail. Secondary antibodies were FITC-conjugated anti-mouse IgG or Texas red–conjugated anti-rabbit or anti-guinea pig IgG (Jackson ImmunoResearch Laboratories, West Grove, PA). Antibodies used are indicated in lower right of each frame. (*A–D*) Examples of partially collapsed networks. (*E* and *F*) Example of a network that is not collapsed. Note the colocalization of the DPI tail with the endogenous keratin network; note also that the DPI tail is absent from endogenous desmosomes. Bar, 30 μm.

transiently transfected cultures (See Fig. 1 *B*). However, we did notice some diffuse cytoplasmic anti-DPI tail staining in very brightly stained cells, suggesting that transient levels may have exceeded binding site capacity within the population. This may have resulted artificially in high levels of DPI proteins that were not tightly associated with the keratin cytoskeleton.

Isolation and Purification of Bacterially Derived Human DPI Tail

While the DPI tail coaligns with keratin filaments in simple epithelial cells (Stappenbeck and Gren, 1992) and in epidermal cells (this study), colocalization does not distinguish between a direct or indirect association. To explore the possibility that the DPI tail might directly interact with keratin IFs, we focused our attention towards in vitro assays, which necessitated a purification scheme for the DPI tail. To this end, we first subcloned sequences encoding 847 COOH-terminal amino acids, beginning at domain A of the DPI tail, into the bacterial expression plasmid pET-8C, which has a T7 RNA polymerase promoter sequence located just 5′ from a multiple cloning region (Studier and Moffatt, 1986; Rosenberg et al., 1987). When *Escherichia coli* strain BL21

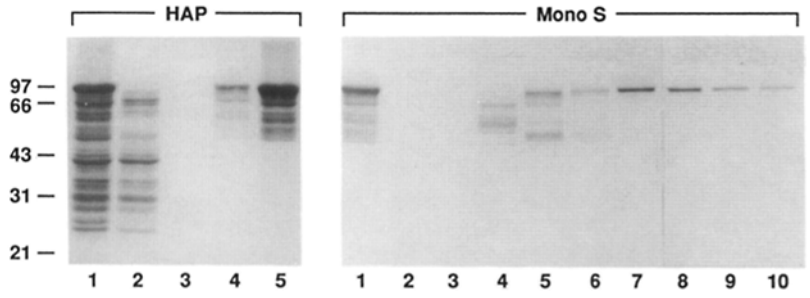

Figure 3. Purification of human DPI tail. Log phase (OD_{600} = 0.6) cultures of pET8c·DPtail bacteria were induced with 1 mM IPTG, and cells were harvested 3-4 h later. IBFs were prepared as described by Kouklis et al. (1993), and the final pellet was solubilized in urea buffer 1 consisting of 6 M urea, 10 mM sodium phosphate, pH 7.8. After centrifugation at 25,000 *g* to remove insoluble material, the protein was then subjected to chromatography on a hydroxyapatite (*HAP*) column equilibrated with urea buffer 1. After extensive washing with urea buffer 1, protein was eluted in 6 M urea, 200 mM sodium phosphate, pH 7.8. The eluent, containing >80% of the total DP tail protein, was then dialyzed against urea buffer 2, consisting of 6 M urea, 50 mM Bicine, pH 8.7, and then loaded onto a Mono S cation exchange column equilibrated in this buffer. The protein was eluted by a 0–500-mM NaCl gradient in urea buffer 2. Aliquots (2-μl) of each of the 500-μl fractions eluted from the gradient were analyzed by SDS-PAGE. Samples from HAP chromatography were: lane *1*, crude IBF preparation; lane *2*, flow through of the column; lane *3*, wash fraction; lane *4*, fraction just after the switch to elution buffer; lane *5*, eluted protein. Samples from Mono S chromatography were: lane *1*, HAP-eluted protein after dialysis; lane *2*, flow through of the column; lanes *3–10*, alternate fractions from the salt gradient, beginning with fraction 9 and ending with fraction 23. Molecular mass standards are shown at left in kilodaltons.

(DE3), harboring a single copy of the T7RNA polymerase gene under the control of the isopropyl-β-thiogalactopyranoside (IPTG)-inducible lac UV5 promoter, was transformed with pET8c·DPtail and subsequently treated with IPTG, large cytoplasmic inclusion bodies (IBs) formed that were not present in untransformed cells.

When solubilized and resolved by SDS-PAGE, inclusion body fractions (IBFs) included a prominent band not present in total bacterial cell extracts (Fig. 3, lane *1*, *upper band*). This band displayed an electrophoretic mobility corresponding to 96 kD, which was in good agreement with the 97-kD mass predicted from the amino acid sequence of the DPI tail. Subsequent immunoblot analysis using an anti-DPI tail monospecific antiserum confirmed the identity of this band (data not shown). Approximately 25–30% of the total IBF consisted of DPI tail or proteolytic fragments thereof.

Intact DPI tail from pET8c·DPtail–transformed cells was purified in two steps, using hydroxy apatite (HAP) column chromatography and Mono S cation exchange (FPLC) chromatography. The DPI tail aggregated under low ionic strength conditions, but it was soluble at 250 μg/ml in phosphate buffered saline, and unless otherwise indicated, the DPI tail was maintained in this buffer. Fig. 3 shows the purity of the DPI tail after (*a*) hydroxyapatite chromatography; and (*b*) cation exchange chromatography. As judged by densitometry scanning of the Coomassie blue–stained gels, the DPI tail was >95% pure after these two columns. As judged by Coomassie blue staining of an overloaded SDS-PAGE gel and subsequent identification by immunoblot analysis (not shown), a slight degradation product of the DPI tail fragment was the only other band detectable in the purified fraction.

A Direct Interaction between the DPI Tail and Type II Epidermal Keratins

When taken together with our immunofluorescence studies, our immunoblot experiments suggested that although the DPI tail associates with the epidermal keratin filament network, this association is not sufficient to withstand sonication in the presence of 1% Triton X-100. To further explore the nature of this interaction, and to assess whether it is a direct or an indirect one, we first determined whether the purified DPI tail was able to associate with assembled keratin filaments in vitro. On its own, the DPI tail remained primarily in the supernatant (S) and not in the pellet (P) when subjected to centrifugation at 27,000 *g* for 2 h at 4°C (Fig. 4). In the presence of a control protein, such as bovine serum albumin, the DPI tail also remained soluble. In contrast, when the DPI tail was added in near stoichiometric amounts to an IF assembly mixture containing the recombinant human epidermal keratins K5 and K14, the assembled keratin IFs, as well as the DPI tail, were quantitatively pelleted

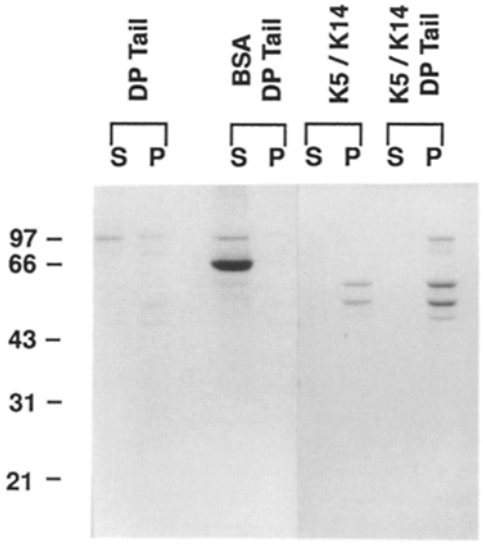

Figure 4. Purified DPI tail cosediments with epidermal keratin filaments. Epidermal keratin filaments were reconstituted in vitro using recombinant human K5 (58 kD) and K14 (50 kD) at 200 μg/ml (see Materials and Methods). The assembly was conducted in the presence or absence of 100 μg/ml DPI tail (97 kD). As controls, assembly reactions were also conducted (*a*) in the presence of DPI tail and the absence of K5 and K14, and (*b*) in the presence of DPI tail and BSA (67 kD). After assembly, the polymerized filaments were sedimented by centrifugation at 27,000 *g* for 2 h. Soluble (*S*) and pellet (*P*) fractions were analyzed by electrophoresis through 12% SDS polyacrylamide gels. Molecular mass standards are indicated at left. Note: During extended polymerization times at room temperature, the DPI tail had a tendency to break down somewhat, but this did not seem to interfere with its ability to associate with K5 and K14.

when subjected to centrifugation (Fig. 4). These findings suggested that in vitro, in the absence of other auxiliary proteins or factors, the DPI tail associated with epidermal keratin filaments when present in physiological buffers.

To further explore the possibility that the DPI tail might directly interact with epidermal keratins, we performed a blot overlay assay (Merdes et al., 1991) using biotinylated DPI tail to probe nitrocellulose blots containing either SDS-PAGE–resolved recombinant IF proteins (Fig. 5 *A*) or IF proteins isolated from various cell types and tissues (Fig. 5 *B*). For both studies, the SDS-PAGE gels are shown at the left and the nitrocellulose blots are shown at the right after probing with biotinylated DPI tail, followed by washing and incubation with horseradish peroxidase–conjugated streptavidin to visualize the binding.

The IF proteins analyzed for DPI tail binding included: Fig. 5 *A*, a mixture of recombinant human K5 and K14 (Coulombe and Fuchs, 1990), recombinant human K6a (gift of P. A. Coulombe, Johns Hopkins University Medical School, Baltimore, MD), and recombinant human vimentin

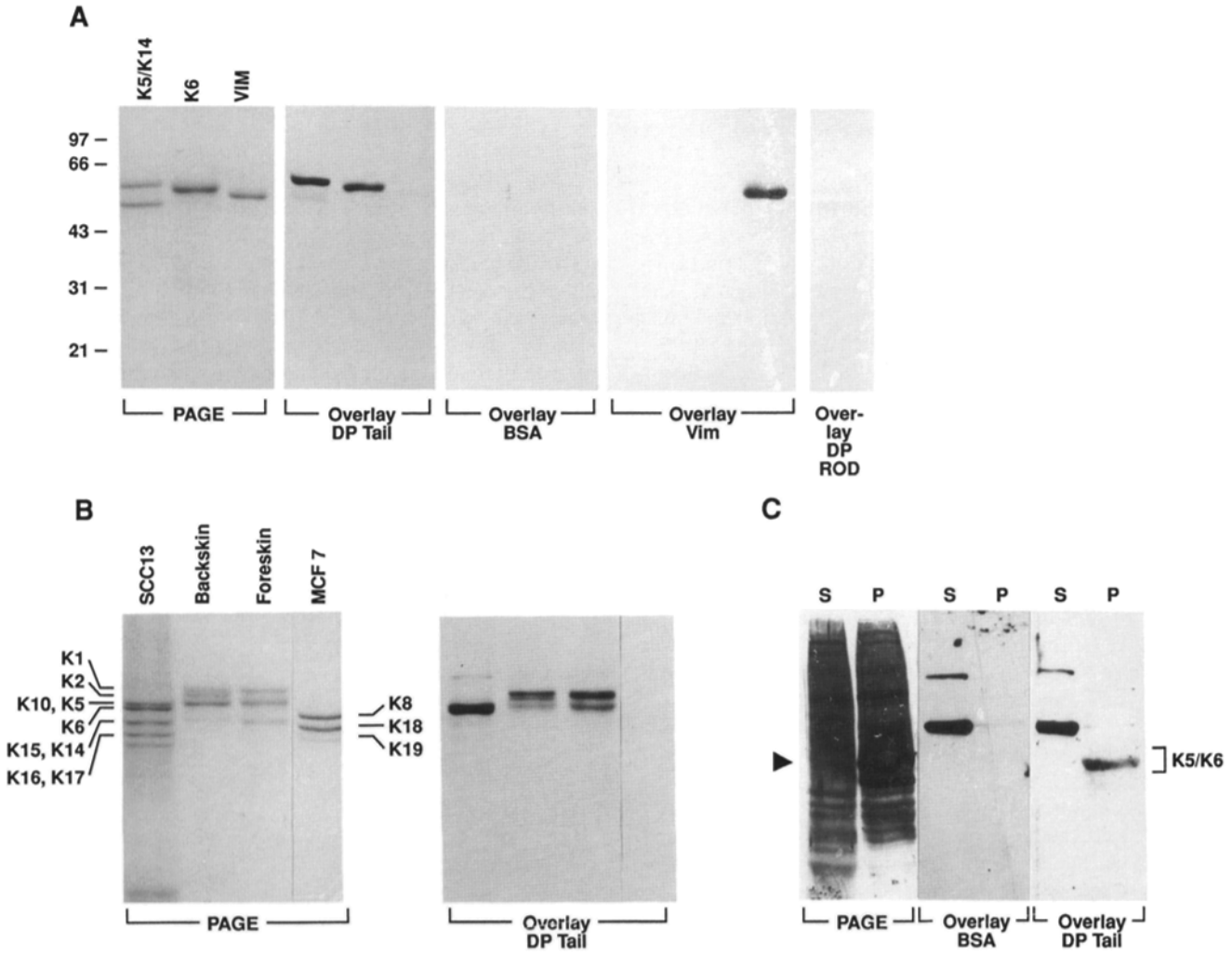

Figure 5. Direct association of the DPI tail with type II epidermal keratins. (*A*) Recombinant human IF proteins, including K5 and K14 (heterodimers isolated by Mono Q fplc), as well as K6 and vimentin, were subjected to electrophoresis through 8.5% SDS polyacrylamide gels and either stained with Coomassie blue (*left*) or transferred to nitrocellulose paper by electroblotting. Blots were then incubated with either DPI tail, BSA, vimentin, or DPI rod segment, each biotinylated as described in the Methods. After binding, blots were washed and processed as described in the Methods. The loading order for blots is the same as that for stained gel, except for the DPI rod segment, where only the K5/K14 complex was tested. Note: K5 (58 kD) and K14 (50 kD) were combined before loading. Note: The faint binding of DPI tail to vimentin is bona fide; the faint hybridizing band in the K5-K14 lane represents a breakdown product of K5, and is not K14. (*B*) IF proteins were extracted from human epithelial cells and tissues as described (Wu et al., 1982), except for SCC-13 IFs, which were extracted in 1% Triton X100 in PBS. For skin samples, epidermis was separated from dermis with 2 M NaBr at 37°C for 15 min. Proteins were resolved by SDS-PAGE and processed as outlined in (*A*). Shown are the Coomassie blue–stained gel and the DPI tail overlay assay for human IF proteins of SCC-13 epidermal keratinocytes, backskin epidermis, foreskin epidermis, and MCF-7 breast adenocarcinoma cells. Keratins are as indicated, according to the nomenclature of Moll et al. (1982). (*C*) Triton X-100–soluble and –insoluble extracts from SCC-13 keratinocytes were overloaded and subjected to SDS-PAGE as above. After transferring to nitrocellulose, one blot was stained with India ink. Identical blots were subjected to overlay assays using either biotinylated BSA as a control, or biotinylated DPI tail. Note: Two major bands, primarily in the soluble fraction but also faint in the insoluble fraction, were artifacts of the streptavidin secondary reagent, and were detected irrespective of the source of the biotinylated protein.

(McCormick et al., 1993); and Fig. 5 *B*, SCC-13 epidermal keratins (K5, K6a/K6b, K14, K15, K16, K17, and K19; Wu and Rheinwald, 1981), backskin epidermal keratins (K1, K2, K5, and K14; Fuchs and Green, 1980; Collin et al., 1992), foreskin epidermal keratins (K1, K5, and K14; Fuchs and Green, 1980; Collin et al., 1992), and MCF-7 keratins (K8, K10, K18, and K19; Moll et al., 1982).

Biotinylated DPI tail bound to recombinant K5 and K6a, but not to vimentin (Fig. 5 *A*, *middle blot*). The smaller, faintly interacting band in the K5 and K14 mixture (*arrowhead*) did not have the same mobility as K14, and was a degradation product of K5, a feature confirmed by running the two recombinant proteins independently (examples are given below). Binding to K5 and K6a was not detected when biotinylated BSA, vimentin, or the DPI rod domain were used as controls (blots at right). Of these, only vimentin showed binding, and as expected, this was to itself.

Biotinylated DPI tail also bound to all type II epidermal keratins, including K1 (67 kD) and K2 (65 kD), as well as K6 (56 kD) and K5 (58 kD) (Fig. 5 *B*). While levels of different type II epidermal keratins varied among samples, making quantitation difficult, binding was roughly comparable to all four keratins. No binding was detected for smaller, i.e., type I epidermal keratins, including K14 (50 kD), K15 (50 kD), K16 (48 kD), K17 (46 kD), and K19 (40 kD). Since K5 comigrated with K10 in the skin extracts, we cannot unequivocally rule out weak binding to K10.

Interestingly, no appreciable binding was detected between the DPI tail and K8 (53 kD), K18 (44 kD), or K19 (40 kD) from human MCF-7 breast carcinoma cells. This was also the case for human LP-9 mesothelial cells (not shown), which express the type II keratin, K7 (55 kD), in addition to the other keratins produced by MCF-7 cells (Wu et al., 1982; Kim et al., 1987). When taken together, our results from sedimentation and overlay assays demonstrated convincingly that the DPI tail and IF proteins can interact directly. Additionally, this reaction appeared to be strongest with the type II epidermal keratins.

To more rigorously test the specificity of the biotinylated DPI tail, we repeated the overlay assays, this time using gels containing overloaded levels of crude Triton X-100–insoluble and –soluble keratinocyte extracts (Fig. 5 *C*). The two major hybridizing bands in the soluble extract were detected by the streptavidin secondary reagent, and were not specific for the DPI tail. Overall, these data convincingly demonstrated that the interaction between the DPI tail and the type II keratins is specific.

Without the Head Domain of a Type II Epidermal Keratin, the DPI Tail Cannot Associate with It

To identify the portion of the type II epidermal keratins involved in direct binding to the DPI tail, we tested binding of the biotinylated tail to a battery of previously engineered truncation mutants of the human K5 polypeptide (for details of K5 mutants, see Wilson et al., 1992). Fig. 6 illustrates the results of this experiment, and its shows the Coomassie blue–stained SDS-PAGE gel (*A*) and the blot overlay assay (*B*). In contrast to full-length K5 that bound the DPI tail strongly (Fig. 6 *B*, lane *1*), K5NΔ71, missing 71 amino acids of the amino terminal head domain, bound the DPI tail only weakly (Fig. 6 *B*, lane *2*). K5NΔ157, missing the entire head domain, exhibited no appreciable binding of the DP tail (Fig. 6 *B*, lane *3*). Similarly, headless and tailless K5, missing both head and tail domains, showed no appreciable interaction with the DPI tail in this ligand-blot assay (Fig. 6 *B*, lane *4*). However, two tailless mutants, K5CΔ117 and K5CΔ111, missing the 111-residue COOH-terminal tail of K5, displayed DPI tail binding that was indistinguishable from wild-type (Fig. 6 *B*, lanes *5* and *6*, respectively; compare with wild-type in lane *1*). Collectively, these data suggested that without the head domain, the ability of the type II epidermal keratins to interact specifically with the DPI tail is lost.

Expression and Purification of the K5 Head Domain and Demonstration that the Head Contains Sufficient Information to Confer Binding to the DPI Tail

A priori, the loss of DPI tail binding as a consequence of removing the keratin head domain does not necessarily imply that the K5 head domain contains sequences sufficient for DPI tail binding. To test this possibility, purification of the K5 head domain was necessary. In this case, sequences spanning the ATG translation start codon (i.e., codon 1) to codon 168 of the human K5 protein (Lersch et al., 1989) were subcloned into the bacterial expression vector pET22b, containing six histidine codons and a TGA stop codon in frame and just 3′ to the K5 sequences. This enabled a one step nickel column purification of the K5 head starting from solubilized IBF proteins (Fig. 7). The electrophoretic mobility of the purified K5 head protein was 20 kD, in good agreement with

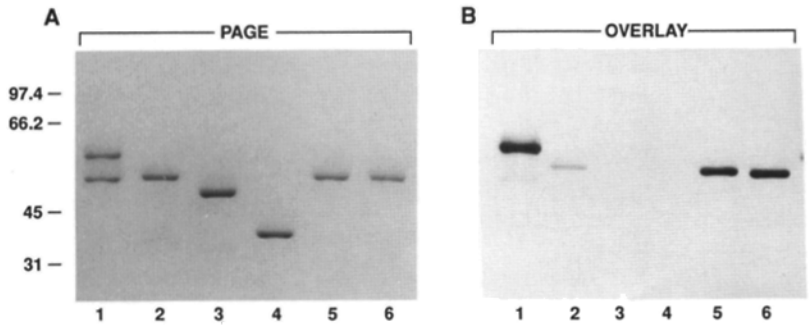

Figure 6. Removal of the head domain abolishes the binding of K5 to the DPI tail. Head and tail mutants of recombinant human K5 (Wilson et al., 1992) were resolved by SDS-PAGE and subjected to the filter-immunobilized, ligand-binding assay with biotinylated DPI tail. Shown at left is Coomassie blue–stained gel and at right the overlay assay of: lane *1*, K5/K14 mixture; lane *2*, K5NΔ71, missing 71 residues from the NH_2 terminus; lane *3*, K5NΔ157, missing the entire NH_2-terminal head domain; lane *4*, K5HT, missing the entire head and tail domains; lane *6*, K5CΔ117, missing the entire COOH-terminal tail; and lane *7*, K5CΔ111, missing 111 amino acid residues from the COOH terminus. Molecular mass standards are indicated at left.

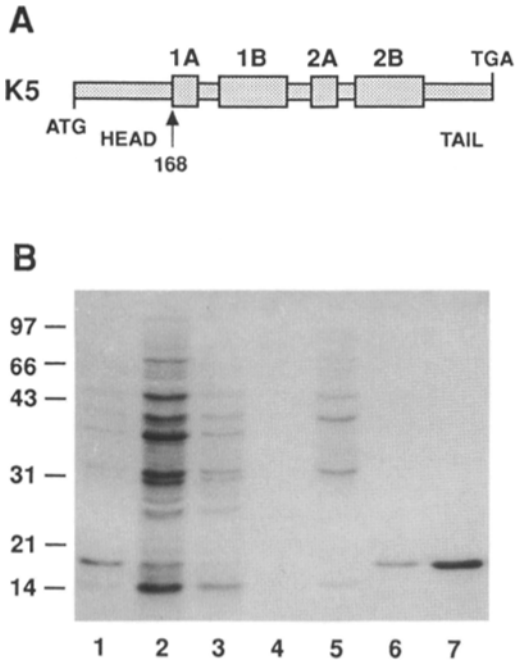

Figure 7. Purification of the human K5 head domain. A Novagen kit was used to purify the K5 head from overnight, IPTG-induced cultures of pET26·K5H bacteria. Note: the leader sequence in the construct was deleted, so the protein remains in the cytoplasm. Briefly, inclusion bodies were purified and solubilized in the recommended buffer that contained 6 M urea. The protein was subjected to affinity chromatography through a nickel ion column, and after washing, the K5 head was eluted with 300 mM imidazole. Lanes *1*, isolated inclusion body fraction (IBF); lane *2*, flow-through material from nickel column chromatography; lanes *3–5*, sequential washes with 5–40 mM imidazole buffer; lanes *6–7*, purified K5 head eluted with 300 mM imidazole. Markers at left indicate migration of molecular mass standards.

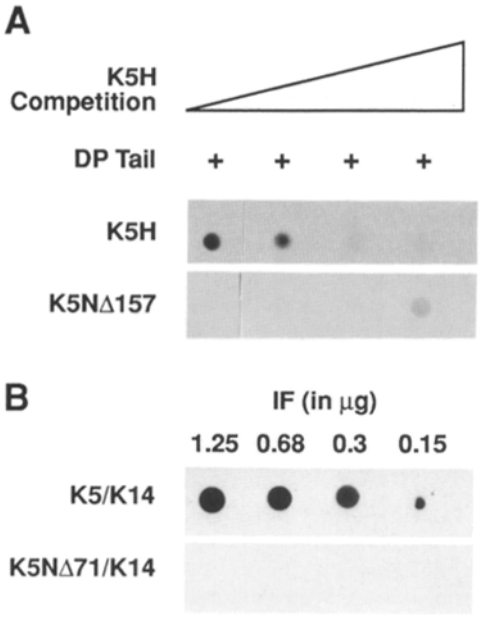

Figure 8. The K5 head associates with the DPI tail directly, on blots, in solution, and when K5 is assembled into IFs. (*A*) Purified K5 head (test; 0.7 μg/sample) and K5NΔ157 (1.2 μg/sample) were transferred to nitrocellulose paper using a dot blot apparatus. Binding reactions with the biotinylated DPI tail (0.25 μg/ml) were then carried out in the absence or presence of unlabeled K5 head at the following concentrations: 0, 0.1, 0.4, and 0.8 μg/ml (*left to right*). After binding reactions, blots were washed and processed as described in Materials and Methods. Note: When very high levels of unlabeled K5 head were added to the binding assay, the DPI tail seemed to show some weak binding to K5NΔ157, perhaps as a consequence of an indirect interaction involving the K5 head. (*B*) Recombinant human K14 was combined with either K5 or K5NΔ71, purified as a complex (200 μg/ml), and assembled into filaments as described in the Methods. After assembly, IFs were spotted onto nitrocellulose paper and were subjected to an overlay assay with biotinylated DPI tail.

that predicted by amino acid sequence. As judged by densitometry scanning, the K5 head was >98% pure.

To test whether the purified K5 head interacted with the DPI tail, we spotted equimolar amounts of headless K5 (NΔ157) and the K5 head (K5H) on nitrocellulose paper and subjected the dot blot to an overlay binding assay with biotinylated DPI tail. As shown in Fig. 8 *A*, the DPI tail bound to the K5 head under conditions where no association with the headless K5 occurred. The level of DPI binding to the purified K5 head was comparable to that which we had previously observed with filter-immobilized wild-type K5. The results were not appreciably different when the ionic strength of the binding buffer was increased to 1.5 M, suggesting that the association does not depend on electrostatic interactions (data not shown). Moreover, binding of the DPI tail to the K5 head was still appreciable when 3 M urea was added to the binding buffer (not shown). Finally, the association also took place in solution, as judged by the ability of competitor K5H in solutin to block the binding of the DPI tail to nitrocellulose-immobilized K5H (Fig. 8 *A*). Collectively, these studies provided direct evidence that it is the head domain of the epidermal type II keratins that contains the information necessary for interaction with the DPI tail.

If the head domain of K5 is physiologically important in binding to the DPI tail, then it must be accessible when in the context of filaments. While our cosedimentation data in Fig. 4 suggest that this is the case, we tested this possibility directly by overlay assays. Wild-type K14 was combined with either (*a*) wild-type K5 or (*b*) K5NΔ71, and it was subjected to filament assembly under conditions where both mixtures assemble efficiently into IFs (Wilson et al., 1992). These IFs were then spotted directly on nitrocellulose, and were subjected to the overlay assay with biotinylated DPI tail. As shown in Fig. 8 *B*, filaments assembled from wild-type K5 and K14 showed marked binding to the DPI tail. In contrast, no appreciable binding was seen with filaments assembled from K5NΔ71 and K14, consistent with our results in Fig. 6, showing that most of the binding was lost when 71 amino acids were removed from the amino end of K5. Collectively, these data provide additional evidence that the K5 head is accessible in the 10-nm filament, and that in this context, it is the domain interacting with the DPI tail.

The Central Portion of the K5 Head is Important for the DPI Tail Binding Activity

Fig. 9 illustrates the sequence of the human K5 head domain. To further define the portion of the type II epidermal head domain involved in the interaction with the DPI tail, we first

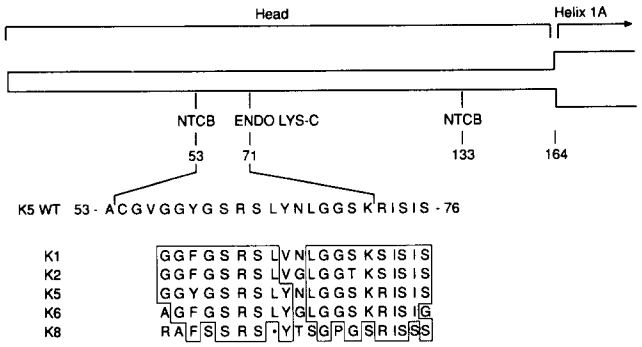

Figure 9. Enzymatic and chemical cleavage sites within the K5 head domain. Shown at top is a stick diagram indicating the junction between the 164 residue head domain and the start of helix 1A of the coiled-coil rod domain of K5. The recombinant K5 head included an additional four residues, followed by a six-residue histidine tag. Shown are the sites of cleavage for the chemical reagent NTCB and the endolysine C protease. Also shown is the sequence from residues 53–76, as well as its conservation among type II keratins. The dot in K8 sequence denotes natural absence of the leucine.

subjected the purified K5 head domain to 2-nitro-5-thiocyanatobenzoic acid (NTCB), which cleaves NH_2-terminal to cysteine residues, and we then tested the resulting polypeptides in the overlay binding assay. The digest was only a partial one, cleaving ~60% NH_2-terminal to cysteine 54, with little or no cleavage NH_2-terminal to cysteine 134 (Fig. 10 *A*, Coomassie blue–stained gel, compare lane *1*, intact, with lane *2*, NTCB digestion). However, it was very clear from the overlay binding assay in Fig. 10 *B* that the ~13 kD, 110–amino acid NTCB peptide (residues 54–164 of the K5 head) still bound to the biotinylated DPI tail in a fashion indistinguishable from the intact head (lanes *1* and *2*, respectively).

To further define the K5 head sequences important for DPI tail–binding activity, we used endolysine protease (ENDO LYS-C), which cleaves COOH-terminal to lysine residues, to generate 93 and 71 amino acid polypeptides (Fig. 10 *A*, lane *3*; ~11 and 9 kD, respectively). Since electrophoretic transfer of these smaller sized peptides to nitrocellulose was not efficient, we separated the two ENDO LYS-C bands by nickel column chromatography. Bound and flow-through fractions were then spotted on nitrocellulose paper and hybridized with the biotinylated DPI tail (Fig. 10 *C*). Both peptides exhibited some binding with the DPI tail, although of the two, the 71-residue peptide corresponding to the amino terminal half of the K5 head (flow-through) displayed markedly stronger (>6×) binding than the 93 residue peptide (bound). This result is consistent with our previous finding that K5NΔ71 bound the DPI tail only weakly (see Fig. 6). When taken together with the NTCB data, these results suggest that residues 54–71 of the K5 head contain information critical for efficient DPI association. This said, there may be additional sequences within the head that also play a role in binding.

Discussion

A Direct Association between IFs and DPI

We have extended earlier in vivo studies by Stappenbeck and Green (1992) and Stappenbeck et al. (1993) to show that the DPI tail interacts with keratin networks of desmosome-rich epidermal keratinocytes. In addition, our in vitro studies, first with sedimentation assays and then with overlay binding assays, provide the first data that directly link the DPI tail with an IF network. These findings are in contrast to those of O'Keefe et al. (1989), who did not observe cosedimentation between keratin filaments and DPI that had been isolated

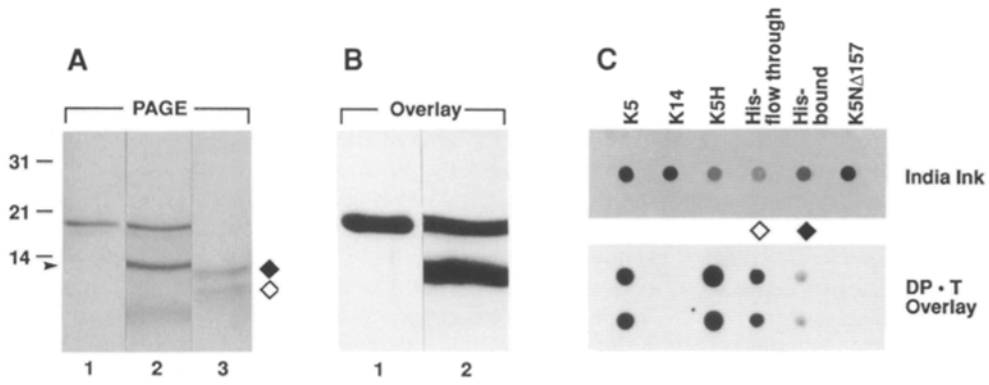

Figure 10. Sequences extending from an NTCB site to an endolysine C site in the K5 head domain are important for DPI tail binding. Recombinant K5 head protein (lane *1*) was subjected to (*a*) chemical cleavage using the cysteine-specific reagent NTCB (lane *2*) or (*b*) enzymatic cleavage using endolysine C protease (lane *3*). For NTCB digestions, 30 μg of K5 head in 40 mM Tris-HCl, pH 8.0, 1 mM EDTA, was subjected to digestion with 2 mM NTCB. After 40 min at room temperature, the pH was adjusted to 9.0 with Tris base, and the digestion was allowed to proceed for an additional 6 h at 37°C. For endolysine C digestion, 125 μg K5 head in 500 μl 2M urea buffer was digested with 0.3 U endolysine C protease for 2 h at 37°C. After digestion, the head fragments were resolved by electrophoresis through 15% SDS polyacrylamide gels and stained with Coomassie blue to visualize the fragments (*A*). Note that the NTCB digest was a partial, generating a 110-residue carboxy terminal fragment (*solid arrowhead*) and a 53-residue amino terminal fragment (diffuse band in lane 2 of *PAGE*). The 133-residue NTCB site did not appear to be cleaved appreciably in this assay. Endolysine C protease cleavage was quantitative, generating a 93- (*solid diamond*) and a 71- (*open diamond*) residue fragment. The K5 head and the NTCB fragments of the K5 head were subjected to an overlay assay using biotinylated DPI tail (*B*). The full-length head and the 110-residue carboxy portion of the head showed binding. The endolysine C protease fragments were subjected to nickel ion affinity chromatography to separate the bound 93-residue histidine tagged fragment from the flow-through 71 residue fragment. After separation, the fragments were transferred to nitrocellulose in triplicate using a dot blot apparatus (*C*), and were tested for either protein level with India ink or DPI tail binding with biotinylated probe (shown in duplicate). K5, K14, and K5NΔ157 were used as controls. Note that the flow-through 71-residue fragment contained the majority of the binding activity. Molecular mass standards are in kilodaltons at left.

and purified from bovine tongue. It is possible that the purification of intact DPI from the desmosomal plaque causes a change in DPI conformation, which in turn affects the tail in a manner that masks or alters its IF binding capacity. Such a change could be physiologically important at times when desmosomes internalize and DPI becomes soluble (see for example, Duden and Franke, 1988). It is also possible that the recombinant DPI tail that we used differs from the corresponding domain of the purified, endogenous DPI used by O'Keefe (1989). In this regard, either phosphorylation or loss of a small but critical portion of the DPI tail during purification might change its binding properties. Further studies will be necessary to fully understand the nature of these differences.

While the DPI tail clearly associates with the keratin network in keratinocytes, it does not associate tightly in vivo, and can be removed by extraction and sonication in the presence of 1% Triton X-100. This said, we were able to recapitulate binding to reconstituted filaments in vitro and to purified K5 head in solution and on blots, thereby demonstrating that the association can be a direct one. We don't yet know whether DPI might be in a different phosphorylation state in vivo that gives rise to a less stable association, or whether accessory proteins might be needed to provide greater stability to this association when it is localized at the desmosomal plaque. In this regard, it is interesting that band 6, a desmosomal protein expressed suprabasally in the epidermis, can associate with the type I simple epithelial keratin K18 in vitro (Kapprell et al., 1988).

Epidermal Type II Keratins Preferentially Associate with the DPI Tail

Intriguingly, our overlay assays revealed an association between the DPI tail and type II epidermal keratins under conditions where no such binding is seen with type I keratins of any source, with type II keratins from simple epithelial cells, or with vimentin. Given the studies of Stappenbeck and Green (1992) and Stappenbeck et al. (1993), we know that in vivo, the DPI tail can associate with simple epithelial keratin networks and with vimentin. How do we resolve this difference?

Several points are worth considering. First, in contrast to some cell types where type III IFs associate with desmosomes (Kartenbeck et al., 1983, 1984; Tokuyasu et al., 1983*a*, 1983b), ~5–10% of SCC-13 epidermal keratinocytes express vimentin and form an independent vimentin IF network that does not associate with desmosomes (Kouklis, P., and E. Fuchs, unpublished observation). One possibility to account for the cell type–specific difference in vimentin IF–desmosome affinity is that tissue-specific phosphorylation states of DPI or tissue-specific proteins might influence the connection between DPI and type III IFs (or DPI and simple epithelial keratin IFs). This could result in a cell-specific variability affecting whether or not an IF network will associate with desmosomes. Alternatively, it could be that the affinity of demosplakin for epidermal keratins is simply much greater than it is for other IF proteins, and therefore, in the presence of an epidermal keratin network, other IFs cannot compete for the limited number of DPI proteins in the cell. While our studies do not distinguish between these possibilities, we certainly show that there is a dramatic difference in the relative abilities of IFs to associate with the DPI tail.

Some of the IF sequences that we have identified as being critical for efficient binding to the DPI tail are not present in vimentin, and they are divergent in the simple epithelial keratins as well. Our failure to detect appreciable binding of the DPI tail to vimentin may be relevant to the recent results of Stappenbeck et al. (1993), who observed that a mutant of the DPI tail that is missing the 68 COOH-terminal residues could still associate with vimentin in transfected fibroblasts, but not with keratins in simple epithelial cells. Thus, the sequences within the DPI tail that are required for coalignment with vimentin may differ from those that are required for association with epidermal keratins. This is perhaps not surprising, in light of the existence of tissue-specific isoforms of desmogleins and desmocollins, which in turn could influence the nature of the association between DPI and IFs, particularly if they are additional cell-type specific factors involved in stabilizing these interactions.

The Importance of the Type II Epidermal Keratin Sequences to Disease and to DPI-IF Superstructure

The overlying binding data point to an 18–amino acid sequence in the head of K5 that seems to play a role in DPI tail binding. A survey of IF head sequences indicates that this sequence overlaps largely with a highly conserved stretch of 20 amino acids extending from residues 57 to 76 of the K5 head (Fig. 9). This segment contains a number of residues that are conserved among all type II epidermal keratins, but that are less conserved in K8, and not discernable in vimentin, K7, or in type I keratins. Within the motif, several sequences are worthy of discussion.

The KRIS. Early in our studies, the lysine in this sequence became of particular interest to us because its biotinylation seemed to perturb the ability of the K5 head to associate with unlabeled DPI tail (not shown). Thus, we were especially intrigued when an abstract appeared reporting a mutation (K:I) at the equivalent lysine residue in K1 of a family with the human blistering skin disorder palmoplantar keratoderma (Kimonis et al., 1994).

Of the more than 40 mutations thus far identified in genetic disorders of keratin, the K:I mutation in the K1 head is interesting in that it falls outside domains that have been implicated in IF assembly (Wilson et al., 1992). When mutated in the context of K5, K71:I causes a decrease, but does not ablate, the binding of the K5 head to the DPI tail (data not shown). Additionally, this lysine is a serine in K8, which does not associate with the DPI tail in our overlay assay. While other explanations are plausible, the K71:I mutation in K1 might weaken the association between desmosomes and epidermal keratin IFs, thereby contributing to fragility and hyperkeratosis in the suprabasal layers of the skin. If true, then some cases of this form of PPK may have mutations in the DPI gene, a hypothesis that can now be tested.

The GSRS. We were also intrigued that the type II keratin motif for DPI binding contained the sequence GSRS because the DPI tail also contains a series of five GSRS repeats located 28 residues from its COOH terminus. A deletion that includes this region of the DPI tail ablates the association between the IF network and the DPI tail (Stappenbeck and Green, 1992; Stappenbeck et al., 1993). Among type II keratins, the GSRS sequence is strictly conserved in all type II epidermal keratins, but not in K8, a type II keratin that does not bind the DPI tail efficiently in our overlay assays.

We do not yet know whether the GSRS sequence motifs in the DPI tail are involved in the association with the GSRS motif in the K5 head domain. However, it is worth noting that arginine and serine sequence motifs have been implicated recently in protein–RNA and protein–protein interactions of the regulatory proteins that govern alternative splicing (Amrein et al., 1994). These protein–protein associations cannot be explained by generic interactions between RS domains, and in this regard, flanking residues appear to be critical (Amrein et al., 1994). Although the functional significance of the parallels between these two different sets of protein–protein associations remains to be established, it could be that a specific array of protein–protein contacts mediated through sequence motifs in arginine- and serine-rich domains could control a variety of macromolecular assembly processes within higher eukaryotic cells.

Summary and Remaining Issues

Our data provide a missing link in our understanding of the nature of associations between IFs and desmosomes. The increased stability of binding between the DPI tail and epidermal keratin head allowed us to observe direct binding in vitro, something that has not been possible for studies on other IF-desmoplakin interactions. While our data do not provide unequivocal evidence that the connection we observed in vitro is functional in vivo, the finding that features of palmoplantar keratoma can occur when this type II head motif is mutated lends support to the possible physiological importance of the interaction.

A number of issues remain. Our preliminary mutagenesis studies have not uncovered a point mutation or small deletion in the K5 head that quantitatively obliterates binding to the DPI tail. Thus, the binding site may be determined by a larger number of residues, reminiscent of tertiary protein conformation. Similarly, if we interpret the findings of Stappenbeck and Green (1992) in light of our direct binding studies presented here, it is likely that the sequences within the 860-residue DPI tail that are involved in the association with IFs are also dependent on tertiary conformation. Indeed, computer studies indicate that both the type II epidermal head and the DPI tail are likely to be globular in structure (Conway and Parry, 1988; Green et al., 1992), a feature consistent with this notion. While crystallography will be necessary to provide a precise solution to the nature of the interaction, our ability to produce pure quantities of soluble DPI tail and K5 head now paves the way for this approach.

A very special thank you goes to Dr. Mary Beth McCormick (University of Washington, Seattle, WA) for her extensive work on isolating and characterizing DPI clones before finishing her Ph.D. in the laboratory. We are also grateful to Drew Syder for his help in DNA sequencing, Yiu-mo Chan for his help in the screening and isolation of some of the point mutants, Grazina Traska for her technical assistance in tissue culture, and Phil Galiga for his assistance with artwork and Chuck Wellek for doing the computer imaging for the cover photo. We thank Dr. Pierre Coulombe (Johns Hopkins University Medical School, Baltimore, MD) for his gift of recombinant human K6 protein, and Dr. Magnus Pfahl (La Jolla Research Foundation, La Jolla, CA) for his gift of the mammalian expression vector pECE-FLAG.

This work was supported by grants from the Howard Hughes Medical Institute and from the National Institutes of Health (AR27883).

Received for publication 25 July 1994 and in revised form 7 September 1994.

References

Albers, K., and E. Fuchs. 1987. The expression of mutant epidermal keratin cDNAs transfected in simple epithelial and squamous cell carcinoma lines. *J. Cell Biol.* 105:791–806.

Amrein, H., M. L. Hedley, and T. Maniatis. 1994. The role of specific protein-RNA and protein-protein interactions in positive and negative control of pre-mRNA splicing by transformer 2. *Cell.* 76:735–746.

Angst B.D., L. A. Nilles, and K. J. Green. 1990. Desmoplakin II expression is not restricted to stratified epithelia. *J. Cell Sci.* 97:247–257.

Arnemann, J., K. H. Sullivan, A. I. Magee, I. A. King, and R. S. Buxton. 1993. Stratification-related expression of isoforms of the desmosomal cadherins in human epidermis. *J. Cell Sci.* 104:741–750.

Bradford, M. M. 1976. A rapid and sensitive method for the quantitation of microgram quantities of protein utilizing the principle of protein-dye binding. *Anal. Biochem.* 72:254–259.

Collin, C., R. Moll, S. Kubicka, J. P. Ouhayoun, and W. W. Franke. 1992. Characterization of human cytokeratin 2, an epidermal cytoskeletal protein synthesized late during differentiation. *Exp. Cell Res.* 202:132–141.

Conway, J. F., and D. A. D. Parry. 1988. Intermediate filament structure: 3. Analysis of sequence homologies. *Int. J. Biol. Macromol.* 10:79–98.

Coulombe, P., and E. Fuchs. 1990. Elucidating the early stages of keratin filament assembly. *J. Cell Biol.* 111:153–169.

Cowin, P., H.-P. Kapprell, W. W. Franke, J. Tamkun, and R. O. Hynes. 1986. Plakoglobin: a protein common to different kinds of intercellular adhering junctions. *Cell.* 46:1063–1073.

Duden, R. and W. W. Franke. 1988. Organization of desmosomal plaque proteins in cells growing at low calcium medium. *J. Cell Biol.* 107:1049–1063.

Franke, W. W., S. M. Troyanovsky, P. J. Koch, R. Troyanovsky, B. Fouquet, and R. E. Leube. 1992. Desmosomal proteins: mediators of intercellular coupling and intermediate filament anchorage. *Cold Spring Harbor Symp. Quant. Biol.* 57:643–652.

Fuchs, E., and H. Green. 1980. Changes in keratin gene expression during terminal differentiation of the keratinocyte. *Cell.* 19:1033–1042.

Garrod, D. R. 1993. Desmosomes and hemidesmosomes. *Curr. Opin. Cell Biol.* 5:30–40.

Green, K. J., R. D. Goldman, and R. L. Chisholm. 1988. Isolation of cDNAs encoding desmosomal plaque proteins: evidence that bovine desmoplakins I and II are derived from two mRNAs and a single gene. *Proc. Natl. Acad. Sci. USA.* 85:2613–2617.

Green K. J., D. A. D. Parry, P. M. Steinert, M. L. A. Virata, R. M. Wagner, B. D. Angst, and L. A. Nilles. 1990. Strucure of the human desmoplakins: implications for function in the desmosomal plaque. *J. Biol. Chem.* 265: 2603–2612.

Green, K. J., M. L. A. Virata, G. W. Elgart, J. R. Stanley, and D. A. D. Parry. 1992. Comparative structural analysis of desmoplakin, bullous pemphigoid antigen and plectin: members of new gene family involved in organization of intermediate filaments. *Int. J. Biol. Macromol.* 14:145–153.

Gumbiner, B. M., and P. D. McCrea. 1993. Catenins as mediators of the cytoplasmic functions of cadherins. *J. Cell Sci.* 17(Suppl.):155–158.

Harlow, E., and D. Lane. 1988. Labelling antibodies. *In* Antibodies: A Laboratory Manual. Cold Spring Harbor Laboratories, Cold Spring Harbor, NY. pp. 340–341.

Jones, J. C., and K. A. Grelling. 1989. Distribution of desmoplakin in normal cultured human keratinocytes and in basal cell carcinoma cells. *Cell Motil. Cytoskeleton.* 13:181–194.

Kapprell, H.-P., K. Owaribe, and W. W. Franke. 1988. Identification of a basic protein of M_r 75,000 as an accessory desmosomal plaque protein in stratified and complex epithelia. *J. Cell Biol.* 106:1679–1691.

Kartenbeck, J., W. W. Franke, J. G. Moser, and U. Stoffels. 1983. Specific attachment of desmin filaments to desmosomal plaques in cardiac myocytes. *EMBO (Eur. Mol. Biol. Organ.) J.* 2:735–742.

Kartenbeck, J., K. Schweichheimer, R. Moll, and W. W. Franke. 1984. Attachment of vimentin filaments to desmosomal plaques in human meningiomal cells and arachnoidal tissue. *J. Cell Biol.* 98:1072–1081.

Kelly, D. E. 1966. Fine structure of desmosomes, hemidesmosomes, and an adepidermal globular layer in developing newt epidermis. *J. Cell Biol.* 28:51–72.

Kemler, R. 1993. From cadherins to catenins: cytoplasmic protein interactions and regulation of cell adhesion. *Trends Genet.* 9:317–321.

Kim, K.-H., V. Stellmach, J. Javors, and E. Fuchs. 1987. Regulation of human mesothelial cell differentiation: opposing roles of retinoids and epidermal growth factor in the expression of intermediate filament proteins. *J. Cell Biol.* 105:3039–3051.

Koch, P. J., M. D. Goldschmidt, R. Zimbelmann, R. Troyanovsky, and W. W. Franke. 1992. Complexity and expression patterns of the desmosomal cadherins. *Proc. Natl. Acad. Sci. USA.* 89:353–357.

Kouklis, P. D., M. Hatzfeld, M. Brunkener, K. Weber, and S. D. Georgatos. 1993. In vitro assembly properties of vimentin mutagenized at the β-site tail motif. *J. Cell Sci.* 106:919–928.

Lersch, R., V. Stellmach, C. Stocks, G. Giudice, and E. Fuchs. 1989. Isolation, sequence and expression of a human keratin K5 gene: transcriptional regulation of keratins and insights into pair-wise control. *Mol. Cell Biol.* 9:3155–3168.

McCormick, M. B., P. Kouklis, A. Syder, and E. Fuchs. 1993. The roles of the rod end and the tail in vimentin IF assembly and IF network formation.

J. Cell Biol. 122:395–407.
Merdes, A., M. Brunkener, H. Horstmann, and S. D. Georgatos. 1991. Filensin: a new vimentin-binding, polymerization-competent, and membrane-associated protein of the lens fiber cell. *J. Cell Biol.* 115:397–410.
Miller, K., D. Mattey, H. Measures, C. Hopkins, and D. Garrod. 1987. Localisation of the protein and glycoprotein components of bovine nasal epithelial desmosomes by immunoelectron microscopy. *EMBO (Eur. Mol. Biol. Organ.) J.* 6:885–889.
Moll, R., W. Franke, D. Schiller, B. Geiger, and R. Krepler. 1982. The catalog of human cytokeratins: patterns of expression in normal epithelia, tumors and cultured cells. *Cell.* 31:11–24.
O'Keefe, E. J., H. P. Erickson, and V. Bennett. 1989. Desmoplakin I and desmoplakin II: purification and characterization. *J. Biol. Chem.* 264:8310–8318.
Pasdar, M., K. A. Krzeminiski, and W. J. Nelson. 1991. Regulation of desmosome assembly in MDCK epithelial cells: coordination of membrane core and cytoplasmic plaque domain assembly at the plasma membrane. *J. Cell Biol.* 113:645–655.
Pasdar, M., and W. J. Nelson. 1988. Kinetics of desmosome assembly in madin-darby canine kidney epithelial cells: temporal and spatial regulation of desmoplakin organization and stabilization upon cell-cell contact. II. Morphological analysis. *J. Cell Biol.* 106:687–695.
Rosenberg, A. H., B. N. Lade, D.-S. Chiu, S.-W. Lin, J. J. Dunn, and F. W. Studier. 1987. Vectors for selective expression of cloned cDNAs by T7 RNA polymerase. *Gene (Amst.).* 56:125–135.
Stappenbeck, T. S., E. A. Bornslaeger, C. M. Corcoran, H. H. Luu, M. L. Virata, and K. J. Green. 1993. Functional analysis of desmoplakin domains: specification of the interaction with keratin versus vimentin intermediate filament networks. *J. Cell Biol.* 123:691–705.
Stappenbeck, T. S., and K. J. Green. 1992. The desmoplakin carboxyl terminus coaligns with and specifically disrupts intermediate filament networks when expressed in cultured cells. *J. Cell Biol.* 116:1197–1209.
Studier, F. W., and B. A. Moffatt. 1986. Use of bacteriophage T7 RNA polymerase to direct selective high-level expression of cloned genes. *J. Mol. Biol.* 189:113–130.
Tokuyasu, K. T., A. H. Dutton, and S. J. Singer. 1983*a*. Immunoelectron microscopic studies of desmin (skeletin) localization and intermediate filament organization in chicken cardiac muscle. *J. Cell Biol.* 96:1736–1742.
Tokuyasu, K. T., A. H. Dutton, and S. J. Singer. 1983*b*. Immunoelectron microscopic studies of desmin (skeletin) localization and intermediate filament organization in chicken skeletal muscle. *J. Cell Biol.* 96:1727–1735.
Virata, M. L. A., R. M. Wagner, D. A. D. Parry, and K. J. Green. 1992. Molecular structure of the human desmoplakin I and II. *Proc. Natl. Acad. Sci. USA.* 89:544–548.
Wilson, A. K., P. A. Coulombe, and E. Fuchs. 1992. The roles of K5 and K14 head, tail, and R/KLLEGE domains in keratin filament assembly in vitro. *J. Cell Biol.* 119:401–414.
Wu, Y.-J., and J. G. Rheinwald. 1981. A new small (40 kd) keratin filament protein made by some cultured human squamous cell carcinomas. *Cell.* 25:627–635.
Wu, Y.-J., L. M. Parker, N. E. Binder, M. A. Beckett, J. H. Sinard, C. T. Griffiths, and J. G. Rheinwald. 1982. The mesothelial keratins: a new family of cytoskeleton proteins identified in cultured mesothelial cells and nonkeratinizing epithelia. *Cell.* 31:693–703.